Am J Transl Res 2019;11(4):1919-1937
www.ajtr.org /ISSN:1943-8141/AJTR0090188

Original Article

Anti-tumor outcome evaluation against non-small cell lung cancer in vitro and in vivo using PolyI:C as nucleic acid therapeutic agent

Yedan Wu[1,2], Wei Huang[2], Liqing Chen[2], Mingji Jin[2], Zhonggao Gao[2], Changshan An[1], Haixiang Lin[3]

[1]Department of Respiratory Medicine, Affiliated Hospital of Yanbian University, Yanji 133000, Jilin, China; [2]State Key Laboratory of Bioactive Substance and Function of Natural Medicines, Department of Pharmaceutics, Institute of Materia Medica, Chinese Academy of Medical Sciences and Peking Union Medical College, Beijing 100050, China; [3]Xinfu (Beijing) Pharmaceutical Technology Co., Ltd, Beijing 100085, China

Received December 20, 2018; Accepted February 24, 2019; Epub April 15, 2019; Published April 30, 2019

Abstract: PolyI:C as a ligand of toll-like receptor 3 has been explored as a nucleic acid therapeutic agent for anti-tumor therapy. The previous PolyI:C studies mainly focused on anti-tumor evaluation at cell level and anti-tumor mechanism involved in MyD88-independent pathway. However, there is a lack of information about the ability of PolyI:C to affect PI3K/Akt/p53 signaling pathway in non-small cell lung cancer (NSCLC), and its pharmacodynamic evaluation in vivo still remain unclear so far. In this study, we explored the anti-tumor mechanism and efficacy in vivo of PolyI:C in NSCLC. Our results showed that PolyI:C had the ability to inhibit tumor cell proliferation and promote cell apoptosis by inducing G1 cell cycle block in LL/2 and A549 NSCLC cells. In vivo animal studies also demonstrated that PolyI:C effectively inhibited the tumor growth, suppressed spontaneous metastasis and prolonged the survival time of LL/2 tumor-bearing mice. Moreover, western blotting and immunohistochemistry assays showed that its anti-tumor mechanism was associated with the interference with PI3K/Akt/p53 signaling pathway. Our results confirmed that PolyI:C increased the expression of CD80, CD86 in spleen dendritic cells of tumor-bearing mice and cytokine secretion in healthy mice. Generally, our study suggests that PolyI:C can become a promising anti-tumor agent.

Keywords: TLR3, PolyI:C, lung cancer, immunotherapy, PI3K/Akt/p53, cytokines, DC

Introduction

Lung cancer is the leading type of cancer deaths and related deaths account for 30% of all cancer deaths. Non-small cell lung carcinoma (NSCLC) is the most common type of lung cancer, accounting for about 85% of this cancer type [1]. Most patients do not survive 5 years after diagnosis, due to advanced metastasis at the time of discovery [2]. In recent years, although targeted therapies have benefited certain subtypes of NSCLC, disease mortality is still high due to chemotherapy drug resistance. It is now recognized that the immune system has the potential to destroy cancer cells and inhibit cancer cell growth through their innate and adaptive responses [3]. The innate immune response is mediated by antigen presenting cells (APCs), such as dendritic cells (DCs), which secrete inflammatory cytokines to induce the apoptosis of cancer cells [4]. With the rapid development of immunotherapy such as PD1, there is a new hope for patients with lung cancer. Recently, immunetherapeutics with high correlation with NSCLC are constantly being discovered.

Toll-like receptors (TLRs) are the most important trans-membrane receptors in innate immunity and are involved in the induction and regulation of immune responses [5]. The latest research has suggested that TLRs found in various tumor cells, which relate them to cancer development and progression [6]. Some types of TLRs detect tumor antigens and arouse primary anti-tumor immune response [7]. TLRs can further prevent the formation of inflammatory tumor microenvironment by eliminating tumor antigens [8]. TLR3 is located in the membrane of endosomes, utilizes a MyD88-independent pathway and recruits TIR-domain-containing adapter-inducing interferon-β (TRIF) to activate AP-1, NF-κB and interferon regulatory factors (IRFs) [5]. Recent evidence suggested

that TLR3 works as a possible therapeutic target in pharyngeal, breast, ovarian, head and neck, prostate, oral squamous cancer [9-15]. PolyI:C is a ligand for TLR3 that activates TLR3, protein kinase RNA (PKR), retinoic acid-inducible gene-1 (RIG-1), and melanoma differentiation-associated protein 5 (MDA5), induces cancer cell apoptosis directly and destroys the tumor microenvironment. In addition, polyI:C was shown to enhance the immunogenicity of tumor antigens by affecting DC maturation and type I interferon (IFN) [16]. These evidences indicate that TLR3 may be used as a therapeutic target in immunotherapy of lung cancer.

PI3K/Akt plays an essential role in the regulation of cell proliferation, inhibition of apoptosis, promotion of metastasis, and correlating with poor prognosis of cancer. Accordingly, blocking the Akt signaling pathway has been the target of anti-cancer therapies. The gene p53 was known as a tumor suppressor gene downstream of Akt but new insights into p53 and TLR suggest that p53 regulates TLR signaling in cancer cells, inhibiting proliferation of cancer cells [17]. Another study showed that polyI:C may cause prostate cancer apoptosis via the PI3K/Akt signaling pathway [18].

Previous study on the anti-tumor mechanism of polyI:C in lung cancer mainly focuses on the MyD88-independent pathway *in vitro*. However, there is a lack of information about the ability of polyI:C to affect signaling proteins of the PI3K/Akt/p53 pathway in NSCLC. Additionally, the pharmacodynamic evaluation of polyI:C *in vivo* still remain unclear. Therefore, in this paper, we not only evaluated the anti-tumor effect of polyI:C by using LL/2 and A549 cells *in vitro*, but also evaluated the anti-tumor and anti-metastasis efficacy *in vivo* in an animal tumor model. Most importantly, we also explored whether its anti-tumor mechanism is related to the interference with PI3K/Akt/p53 signaling in lung cancer. Moreover, as DC maturation is a key issue in cancer immunotherapy, we also analyzed CD80 and CD86 of spleen DC cells in lung cancer model mice.

Materials and methods

Materials

The PolyI:C preparations used in this study, named as Pamica (Ltd 20171101), were provided by Xinfu (Beijing) Pharmaceutical Technology Co., Ltd. The PD1 (BE-0033-2-25MG) were provided by BioXcell. CCK8 kit was provided by DOJINDO; Annexin V-FITC Apoptosis Detection kit was provided by Neobioscience; TUNEL-POD kit was provided by Leica. All other reagents are of analytic grade.

Two lung adenocarcinoma cell lines, murine LL/2 and human A549 cell lines were received from the Cell Culture Center of Institute of Basic Medical Sciences in Chinese Academy of Medical Sciences. Cells were grown in DMEM medium supplemented with 10% FBS and 1% penicillin/streptomycin. All cells were incubated in a cell culture chamber containing 5% CO_2 at 37°C.

RT-QPCR analysis

The harvested cells were lysed with Trizol reagent (Invitrogen), digesting DNA from sample RNA with DNase I (Fermentas). RNA reversed transcription to cDNA using M-MLV. Real time qPCR was performed with 2 × Ex TaqMix, using a Roche Light Cycler® 480II under the following conditions: 95°C for 5 min, 95°C 15 s→65°C 30 s (fluorescence detection), 45 cycles. The primers used for RT-QPCR were as follows: TLR3, 5'-CCAGACCTAGCACAACTGACTCC-3' (forward) and 5'-AGCAGCCAGAAGCAGAACTACAGA-3' (reverse); β-actin, 5'-GAGATTACTGCTCTGGCTCCTA-3' (forward) and 5'-GGACTCATCGTACTCCTGCTTG-3' (reverse). The qPCR products were analyzed in triplicates. Analysis of relative gene expression data was calculated using the $2^{-\Delta\Delta CT}$ method.

Cell viability assay

LL/2 cells and A549 cells were seeded in 96-well plates at a concentration of 7×10^3 cells/well and 5×10^3 cells/well, and were placed in DMEM medium containing 10% FBS and maintained in a 37°C incubator for adhesion. After 24 h, replaced the medium in all wells with fresh medium containing a range of different concentrations of PolyI:C, and set control and blank wells, then cultured for another 24 or 48 hours. Afterwards, the medium of all wells were changed with serum-free medium containing 10% CCK8 reagent (DOJINDO, Japan), and the cells were further cultured in incubator for another 2 hours in the dark. Finally, the absorbance was detected at 450

nm, taking absorbance at 650 nm as a reference value through a Synergy H1 Microplate Reader (BioTek, U.S.A). Cell viability was calculated according to the below equation:

Equation 1: Cell viability (%) = $(OD_{test} - OD_{blank})/(OD_{control} - OD_{blank}) \times 100\%$

Monolayer cell proliferation

The total number of cells was evaluated by monolayer cell proliferation. LL/2 cells and A549 cells were seeded in 6-well plates at a density of 5×10^4 cells/well, and were placed in DMEM medium with 10% FBS and maintained in incubator for adhesion. After 24 h, replaced the medium in all wells with fresh medium containing with DMEM only or 100 μg/mL of PolyI:C and cultivated for 48 hours. The total number of cells was evaluated every 24 hours to assess cell proliferation. Cells in each well were collected, and treated with trypan blue solution (Solarbio, U.S.A.) staining of viable cells, and counted using a hemocytometer.

Annexin V-FITC/PI double staining assay

Apoptosis of LL/2 and A549 cells were quantitatively determined using Annexin V-FITC/PI double staining assay. LL/2 cells and A549 cells were seeded in 6-well plates at a density of 1×10^5 cells/well, and were placed in DMEM medium and maintained in incubator for adhesion. After 24 h, replaced the medium in all wells with fresh medium containing with DMEM only or 100 μg/mL of PolyI:C and cultured for 48 hours. Cells were collected and washed with cold PBS twice, re-suspended with Binding Buffer, labeled with Annexin V-FITC and PI (Neobioscience Annexin V-FITC Apoptosis Detection kit, Neobioscience, China). Apoptotic analysis was performed by FACSAria flow cytometry (BD, U.S.A) with Cell Quest software (BD, U.S.A).

Cell cycle analysis

Cell cycle was analyzed using flow cytometry. LL/2 cells and A549 cells were seeded in 6-well plates at a density of 1×10^5 cells/well. After 24 h, treated with 100 μg/mL of PolyI:C or DMEM as control, and cultured for 48 hours. All cells were harvested and then re-suspended in 75% ethanol maintaining at -20°C for 24 hours. After that, cells were washed with cold PBS twice added 100 μL RNaseA solution (Solarbio, USA) to the cell pellet and re-suspend the cells, treated in a water bath 30 minutes at 37°C. All cells were labeled with 400 μL PI reagent (Solarbio, USA) and incubated 30 min at 4°C in the dark. Finally, FACSAria flow cytometry (BD, U.S.A) was used to detect red fluorescence with excitation wave length of 488 nm.

Scratch wound healing assay

LL/2 and A549 cells were seeded at a concentration of 5×10^4 cells/well in a 12-well plate for 24 hours. The confluent monolayer cells per well was wounded with a 200 μL pipette tip, washed with PBS twice and intervened with a PolyI:C at a concentration of 100 μg/mL. Cells untreated were used as controls. Monitoring migrate to the wound position of the two front gap of 0, 24 and 48 hours the cells, the cells and captures images of the nine fixed position. Gap area was measured using Image J analysis software.

Transwell migration and invasion assays

For the sake of detecting the influence of PolyI:C on migration and invasion ability of lung cancer cells, we used a 24-well cell culture inserts (3422, Corning, U.S.A). For cell migration assay, LL/2 and A549 cells were pre-treated with 100 μg/mL PolyI:C or DMEM for 48 h in a 37°C incubator, respectively. Then cells were harvested, re-suspended in FBS-free DMEM, and added at a density of 5×10^4 cells/well into the upper transwell chambers. Meanwhile, using 10% FBS in the bottom chamber as a chemoattractant and incubated for 24 h. Subsequently, untransformed cells in the upper layer of the membrane were cleaned up. The migrated cells in the underneath of transwell insert were fixed with anhydrous methanol, labeled with crystal violet for 30 min in the dark and photographed in different view fields under a microscope. For invasion assay, the Matrigel was diluted 1:5 in DMEM without FBS and added to the upper chamber, curing overnight in a 37°C incubator, carried out subsequent experiments according to the migration experiment. For quantitative assay, the crystal violet staining cells was dissolved in 33% acetic acid and their optical density values (OD) were measured at 570 nm. The results were normalized to the untreated LL/2 or A549 cells.

Equation 2: Migration (%) = (A_{sample} - A_{blank}/$A_{control}$ - A_{blank}) × 100%

Equation 3: Invasion (%) = (A_{sample} - A_{blank}/$A_{control}$ - A_{blank}) × 100%

Western blot analysis

Added 200 μl of RIPA lysate to cell, shake vigorously, incubated on ice for 20 min, sonicated, 3 min, centrifuged at 13,000 rpm (4 degrees) for 20 min. Protein quantification according to BCA method. 22 μg of protein were loaded and separated on SDS ± PAGE (10%). After transferring to a polyvinylidene fluoride (PVDF) membrane (Millipore, Billerica, MA), the membrane was incubated overnight at 4°C with antibody against p-Akt (1:5000; abcam), Akt1/2 (1:2000; abcam), CyclinD1 (1:1000; abcam), p21 (1:1000; abcam), p53 (1:1000; abcam), Caspase-3 (1:2000; abcam) or mouse monoclonal antibody against β-actin (1:1000; ZS). 5% BSA-TBST diluted secondary antibody, goat anti-rabbit, goat anti-mouse IgG (H+L) HRP (Jackson) 1:10000, incubated for 40 min at room temperature. ECL was added to the protein surface of the membrane for 3 min; film exposure: 10 s-5 min. Relative protein levels were calculated by normalization to β-actin as a loading reference.

Animal studies

Female C57BL/6 mice, 5- to 6-week-old, 16-18 g weight were obtained from Beijing Vital River Laboratory Animal Technology Co., Ltd. Animal care and all experiments were conducted ethically approved by the Principles of Laboratory Animal Ethics Committee of the Institute of Materia Medica in Peking Union Medical College.

Tumor models and treatment protocols

The lung cancer transplantation model mice were randomly divided into four groups (n = 6): PBS group, PolyI:C inhale group, PolyI:C im group and PD1 group. C57 Mice were injected subcutaneously with 1 × 10^6 LL/2 cells into the right flank. The tumor growth was checked daily. When the tumor volume reached 100 mm^3, 100 μL (200 μg) of PolyI:C was given by inhale or im every other day, or 100 μg of PD-1 was given once a week by ip, or 100 μL of PBS was given by inhale every other day. The animals were monitored for tumor volume and weight. The tumor length and width was measured every other day with digital calipers, and calculated tumor volume using the formula V = 0.5 × L × D^2 where V represents tumor volume, L represents tumor length and D represents tumor width. When the average tumor volume of PBS group reached 2000 mm^3 the animals were quickly killed by cervical dislocation. All tumor tissues were excised and weighed for quantitative comparison, and calculated the tumor inhibition rate according to the following formula 4. Then, tumor, lung, liver, brain tissues were fixed in formalin, then paraffin-embedded, spleen tissues were saved in PBS for follow-up experiment.

Equation 4: Inhibition Rate (%) = (Tumor weight-untreated - Tumor $weight_{treated}$)/Tumor $weight_{untreated}$ × 100%

Hematoxylin and eosin staining of organ organization

Lung, liver, brain tissues were sectioned to 5 μm, and stained with hematoxylin and eosin. Histopathological examination of the stained samples was carried out, and the tissue slides were visualized and photographed at 40 × magnifications under a biological microscope (DM4000B, Leica, Germany).

Tunel staining of transplanted tumor tumor

The apoptosis in tumor tissue was detected by TUNEL assay, sectioned to 4 μm, using a TUNEL-POD kit. Histopathological examination of the stained samples was carried out, and the tissue slides were visualized and photographed at 40 × and 200 × magnifications under a biological microscope (DM4000B, Leica, Germany).

Immunohistochemical analysis

Immunocytochemistry was done on formalin-fixed, paraffin-embedded tissue sections (4 μm). Incubated sections with PBS containing 3% hydrogen peroxide for 30 min, then repaired of antigens in paraffin sections by microwave method. Incubated 5% goat serum for 30 min at room temperature, added diluted primary antibody. The next day, incubated the secondary antibody for 2 hours at room temperature. Added DAB and incubated 5 min, rinsed with PBS added hematoxylin dye solution, then

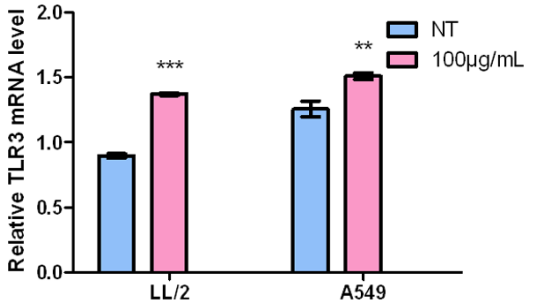

Figure 1. RT-QPCR analysis of relative TLR3 mRNA levels in LL/2 and A549 cells after 48 hours treatment with PolyI:C. NT represents non-treated. Data are expressed as x ± s, n = 3, **P < 0.01, ***P < 0.001.

return to blue with PBS for 5 min. Dehydration: 50% ethanol soak for 1-2 min, 75% ethanol soak for 1-2 min, 95% ethanol soak for 1-2 min; 100% absolute ethanol soak for 1-2 min. Transparent: xylene I is soaked for 1-2 min, and xylene II is soaked for 1-2 min; Neutral gum seals. All tissue slides were visualized and photographed at 200 × magnifications under a biological microscope (DM4000B, Leica, Germany). The primary antibody used in the experiment is as follows, anti-Akt1/2 (Abcam), anti-Akt1 (Abcam), anti-p53 (Abcam), anti-CyclinD1 (Abcam), anti-caspase3 (Abcam), anti-p21 (Abcam).

Flow cytometry assay

The spleen tissue was cut and transferred to a 70 μm cell sieve, immersed in a dish containing 5% FBS in 1640 medium, gently ground with a syringe stopper until the tissue was completely ground into individual cells and filtered through a sieve. Added 5 ml of 1 × RBC Lysis Buffer (10 ×) (BioLegend) and incubated for 10 minutes at room temperature. Then, added CD11c (BioLegend), CD80 (BioLegend), CD86 (BioLegend), I-A/I-E (BioLegend) antibody, incubated for 20 minutes at room temperature. Flow cytometry was carried ona LSRII FACS machine (Becton Dickinson), using analysis software FACS Diva6.0.

Effects of PolyI:C on cytokines in vivo

In order to detect changes in cytokines in the body before and after administration, we used the multiplex immunoassay. Normal healthy C57 were randomly divided into two groups: PBS and PolyI:C im group. 2 h after administration, blood was taken from the posterior venous plexus of the mouse eye, and then quickly killed by cervical dislocation. Separate serum and saved at -80°C for subsequent experiments. The cytokines in serum was detected by Multiplex immunoassay using a ProcartaPlex™ kit according to the manufacturer's protocol.

Survival analysis

Twenty-four LL/2 transplantation model mice were randomly divided into four groups (n = 10): PBS group, PolyI:C inhale group, PolyI:C im group and PD1 group. When the tumor volume reached 100 mm^3, 100 μL (200 μg) of PolyI:C was given by inhale or im every other day, or 100 μg of PD-1 was given once a week by ip, or 100 μL of PBS was given by inhale every other day. Inoculation of mice with LL/2 cells was considered as first day, mice were checked daily until they all died for 50 days.

Statistical analysis

All experiments were repeated three times. All data were expressed as x ± s, using independent-samplet-tests, ANOVA and log-rank analysis. P < 0.05 was considered to be significant. All statistical tests were two-tailed. Statistical analysis and graphs were created using SPSS Statistics 19 (version 4.0.100.1124; SPSS Inc., IBM Company, USA) and GraphPad Prism 5.0 (version 5.0.0.0, GraphPad Software Inc., USA). Image analysis used Image J (64-bit Java 1.8.0_112).

Results and discussion

PolyI:C increased TLR3 expression in LL/2 and A549 cell lines

The pattern of TLR3 gene expression in lung cancer cells may be an indicator of susceptibility to PolyI:C. Hence, we detected TLR3 mRNA levels in mouse LL/2 and human A549 lung cancer cell lines. As shown in **Figure 1**, TLR3 content was detected in both kinds of cells; TLR3 mRNA levels were 0.90 in LL/2 and 1.26 in A549 relative to β-actin. In addition, the TLR3 levels of LL/2 and A549 were elevated to 1.37 and 1.52, respectively, when stimulated with PolyI:C (***P < 0.01, *P < 0.01). We concluded that PolyI:C stimulation increased TLR3 expression in LL/2 and A549.

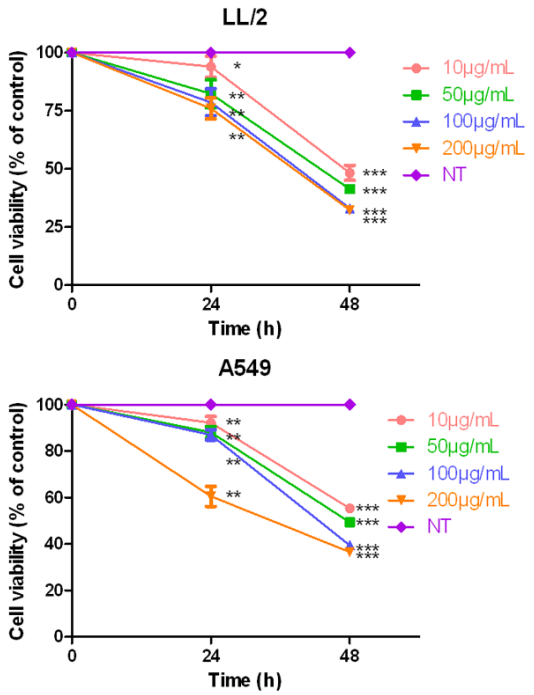

Figure 2. Changes in cell viability of LL/2 and A549 cells after 24 hours and 48 hours treatment with different concentrations (10, 50, 100, 200 μg/mL) of PolyI:C. NT represents non-treated. Data are expressed as x ± s, n = 4, *P < 0.05, **P < 0.01, ***P < 0.001.

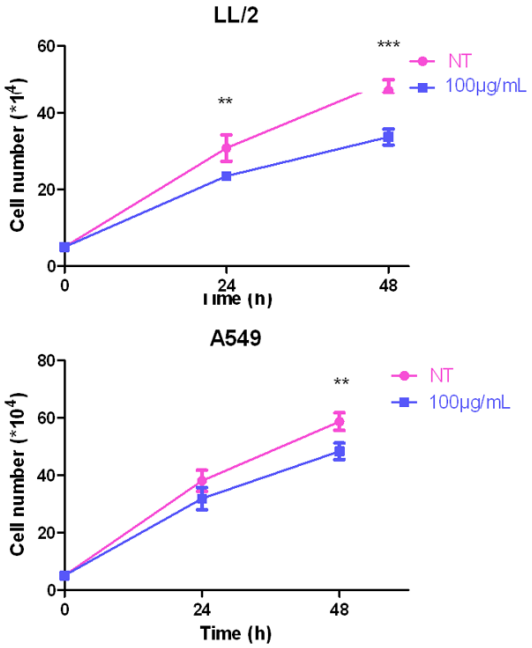

Figure 3. Total cell number was calculated using monolayer cell proliferation. Cells were treated over 48 hours. NT represents non-treated. Data are expressed as x ± s, n = 3, **P < 0.01, ***P < 0.001.

Inhibitory effect of PolyI:C on LL/2 and A549 cell proliferation

We evaluated the influence of PolyI:C on the viability of lung cancer cells using the CCK-8 cell viability assay. According to our results in **Figure 2**, PolyI:C could effectively suppress the viability of both LL/2 and A549 cells at a time-dose-dependent mode within the scope of 10 μg/mL to 200 μg/mL for 48 hours. Concentration-time curve of PolyI:C illustrated that 24 h treatment with 100 μg/mL reached 20% and 13% maximum killing of LL/2 and A549, respectively. After 48 h treatment, LL/2 displayed more dose-dependent cell death with PolyI:C, with 52% and 67% mitigation at 10 and 100 μg/mL PolyI:C, respectively, while A549 was 45% and 61%. These changes reflected the effective inhibition of PolyI:C on LL/2 and A549 cells proliferation. However, increasing PolyI:C dose did not achieve more cell death, hence, 100 μg/mL PolyI:C was used for all follow-up studies.

It is known that, the antitumor effect of PolyI:C is through apoptosis and anti-proliferation on cancer cells [19, 20]. To determine whether PolyI:C reduced cell viability produced in suppression of cell proliferation or induction of cancer cell death, we examined cell monolayer proliferation. We found that cell monolayer proliferation of lung cancer cells could be inhibited by PolyI:C. After 24 h treatment, PolyI:C reduced the monolayer cell number of LL/2 and A549, respectively, to 1.47 and 1.24 times less. However, there was no significant difference in the total number of monolayer cells between the PolyI:C group and the NT group after 24 hours of administration. It can be understood that the inhibition of proliferation of A549 in the PolyI:C within 24 hours was not obvious. Therefore, we continued to study the effect of PolyI:C on monolayer cells for 48 hours. We could observe that PolyI:C suppressed for 2.87 and 2.07 times less of total monolayer cell number in LL/2 and A549 (**Figure 3**). For A549, PolyI:C also significantly inhibited the proliferation of monolayer cells after 48 hours of administration (*P < 0.01). In short, these results demonstrated that PolyI:C could reduce the multiplication time of LL/2 and A549 which may be related to inhibition of cell viability.

Influence of PolyI:C apoptosis and cell cycle

Next we examined apoptosis to further understand the reasons for the decrease in cell via-

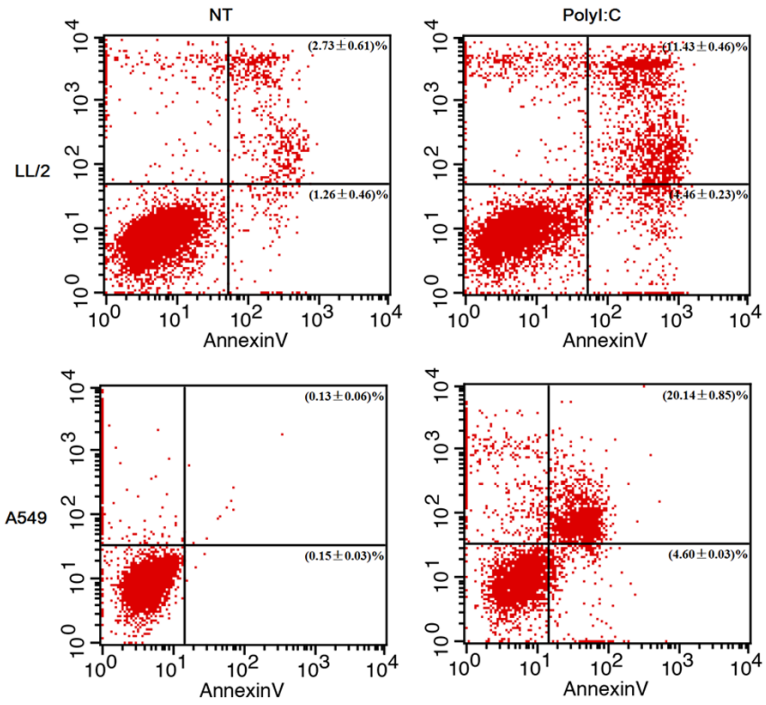

Figure 4. Apoptosis of LL/2 and A549 were determined with Annexin V-FITC/PI staining assay, after 48 hours administration. Data are expressed as x ± s, n = 3.

bility of PolyI:C-treated LL/2 and A549 cells. As shown in **Figure 4**, after PolyI:C treatment for 48 h, late cellular apoptosis was mainly observed (upper right quadrant). The late apoptotic cell ratio of LL/2 and A549 were (11.43 ± 0.46)% and (20.14 ± 0.85)%, respectively, which were significantly increased compared to those in the control groups, (2.73 ± 0.61)% and (0.13 ± 0.06)% (***P < 0.001). In order to observe whether PolyI:C affects the cell cycle, we conducted further studies by flow cytometry with PI staining. As shown in **Figure 5**, cell cycle arrest analysis showed that PolyI:C could accumulate LL/2 cells in G1 phase after 48 hours post-treatment. To the contrary, the cell ratio in S and G2 phases were significantly reduced. The total ratio of LL/2 cells at G1 was (32.01 ± 0.09)% in PolyI:C group while it was (17.11 ± 1.12)% in the control group (***P < 0.001). As far as A549 was concerned, there was also a G1 phase arrest, but not as obvious as LL/2, the G1 phase in PolyI:C group was (55.16 ± 0.97)%, and (46.52 ± 0.58)% in the control group (***P < 0.001). We speculated that PolyI:C could arrest LL/2 cell cycle at G1 phase and induce apoptosis and sequentially inhibit cell proliferation.

Influence of PolyI:C on cell motility in vitro

The migration and invasion of cancer cells can cause them to metastasize to other organs [21]. According to one report, PolyI:C suppresses metastasize in human lung cancer cells [22]. By performing scratch wound healing assay, transwell migration and invasion assays, we displayed the anti-metastatic effects of PolyI:C on LL/2 and A549 *in vitro*. In order to investigate the interfering effect of PolyI:C on the parallel movement of cells, a scratch wound healing assay was carried out. Our results showed that (**Figure 6**), the wound gap in control group was almost completely healed in A549 cells, but in LL/2 cells healing was not obvious, indicating that A549 cells had superior metastatic properties. In the PolyI:C group, the wounds became narrow after 48 h incubation both with LL/2 and A549 cells. After 48 h incubation, the wound area of PolyI:C-treated LL/2 was reduced from 1673025 μm^2 to 902610 μm^2, but in the control group, the value was reduced from 1714904 μm^2 to 749944 μm^2. For A549, the value of untreated was reduced from 1166710 μm^2 to 363945 μm^2, while PolyI:C-treated was reduced from 1067701 μm^2 to 525084 μm^2. Additionally, compared to the control group, the motility of PolyI:C-treated cells were significantly decelerated, especially for A549 cells.

As parallel transfer capability of LL/2 was not obvious, we therefore examined the inhibitory effect on longitudinal movement by PolyI:C on LL/2 and A549 cells with transwell assays (**Figure 7**). As anticipated, cells in the control group crossed the membrane and covered the lower surface, which demonstrated the strong migratory ability of LL/2 and A549 cells. PolyI:C showed a certain degree of inhibition of migration, and the ratio of LL/2 and A549 on the lower surface was (85.80 ± 3.31)% and (82.96 ± 1.27)% (P < 0.05). It is worth pointing out the

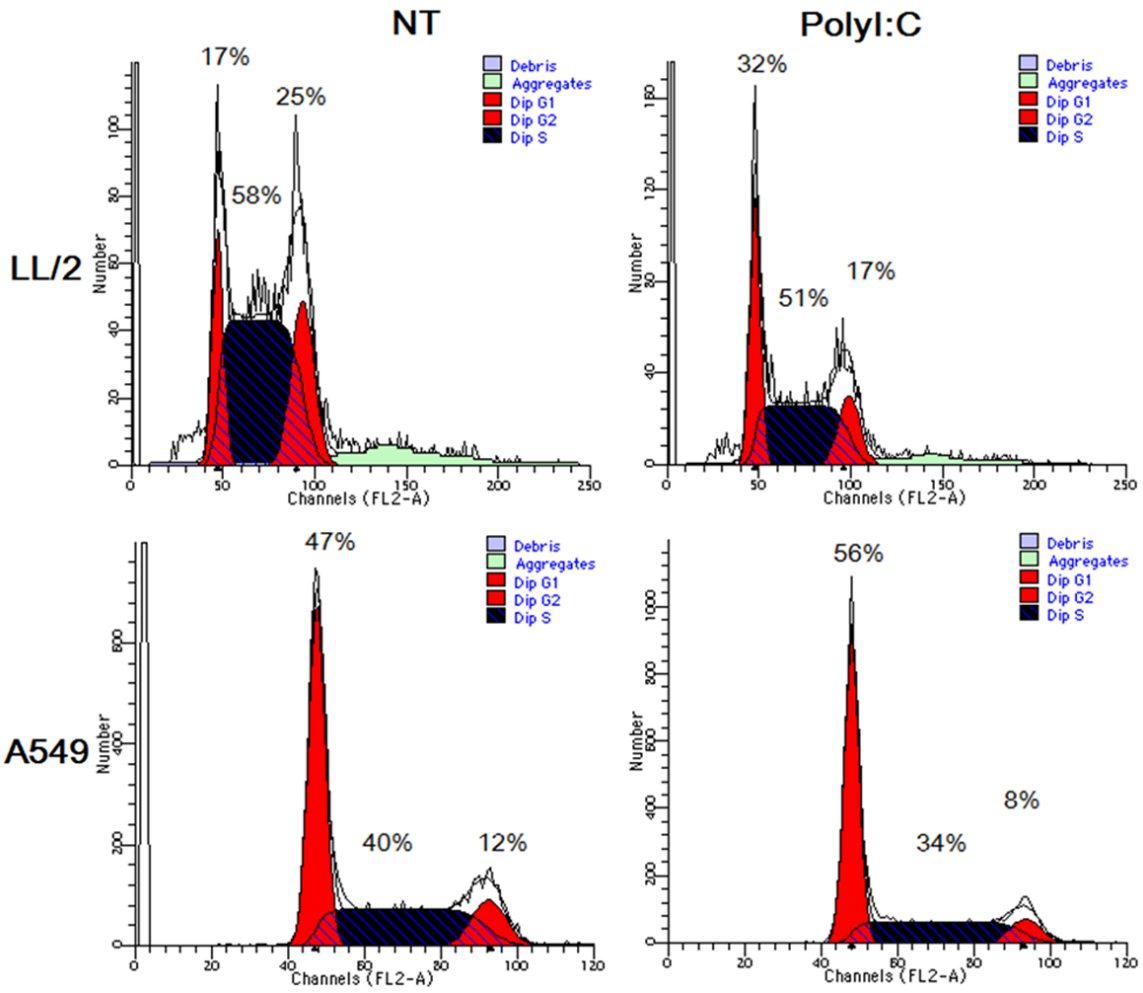

Figure 5. Cell cycle was analyzed by flow cytometry after 48 hours administration. Data are expressed as x ± s, n = 3.

migration ability of LL/2 and A549 cells were significantly inhibited after treatment with PolyI:C. We also examined whether PolyI:C inhibits the invasiveness of lung cancer cells by using matrigel invasion assays. As the figure shows, images of cells on the lower surface of the matrigel membrane, means both kinds of cells had some invasive ability, especially for A549. The cells treated with PolyI:C showed anti-invasive ability in the traversal of matrigel membrane, and the percentages of invasive ability were (58.09 ± 1.34)% in LL/2 and (82.25 ± 2.24)% in A549. These outcomes imply that PolyI:C is resistance to metastatic, it suppressed the metastatic potential of LL/2 and A549 cells, and the inhibition of LL/2 invasion was more obvious.

Anti-tumor effect of PolyI:C in vivo

The antitumor efficacy of PolyI:C against murine lung cancer was investigated to make a thorough inquiry the antitumor potential of PolyI:C *in vivo*. LL/2 cells were planted into the right forelimb armpit of female C57BL/6 mice to establish a murine lung cancer transplanted tumor model. When the tumor volume reached about 100 mm^3, PolyI:C solution and PBS as negative control was respectively administered to tumor-bearing mice for anti-tumor treatment. Moreover, to understand the anti-tumor activity of PolyI:C compared to what is actually used as anti-cancer therapeutic, a well-known anti-cancer agent, PD1 for positive control group. To monitor tumor growth, a Vernier caliper was used to measure tumor volumes every other day. The tumor volume (**Figure 8**) shows that the tumors of mice in PBS group grew very fast, but the tumors in treatment groups resulted slower. Moreover, the results of both im and inhale PolyI:C groups were less than the PD1 group.

After the last measure of tumor volume was completed, the mice were sacrificed and the

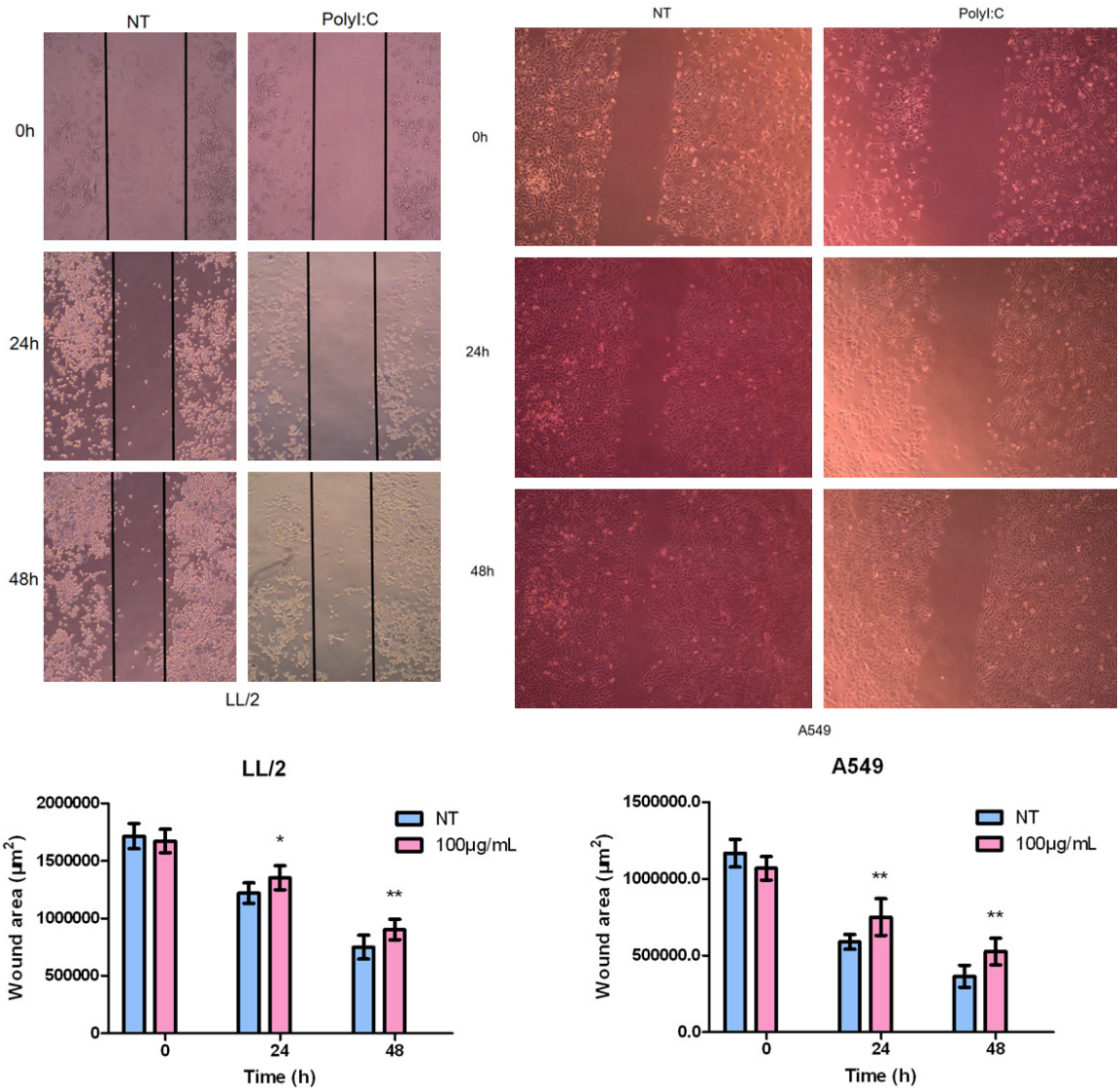

Figure 6. Cell motility measured using wound healing assay after 48 hours administration. Samples were pictured (magnification: × 200) at different time points (0 h, 24 h, 48 h) after treatment. Wound area was analyzed using Image J software (64-bit Java 1.8.0_112), for comparing wound recovery. NT represents non-treated. Data are expressed as x ± s, n = 3, (*P < 0.05, **P < 0.01).

tumor tissues were exfoliated to compare tumor weight. As seen in **Figure 9**, the mean tumor weight in both PolyI:C groups were significantly smaller than that in PBS and PD1 group. The respective inhibition rates of im and inhale groups were 51% and 39%, higher than PD1 group which was 15%. In order to clarify the toxicity of PolyI:C *in vivo*, we monitored the body weight of the mice. We observed weight loss in the mice within the inhale group was not obvious, but from the seventh administration, the weight of mice in the im group decreased significantly, and there was statistical significance (**Figure 8**) (*P < 0.05). From this result, we concluded that a side effect of PolyI:C is weight loss, however, compared with im group, inhale group has poor anti-tumor effect with no weight loss. Finally, TUNEL assay was performed to explore the apoptosis and necrosis in tumor tissues (**Figure 10**). Tumor cell quantity decreased in all treatment groups. More brown cells could also be found in the im group compared to the inhale group, as well as more induced apoptosis and necrosis in tumor tissues and tumor growth inhibition.

Anti-spontaneous metastasis activity of PolyI:C

It is understood that multiple organ metastases often occur in the late stage cancers, and

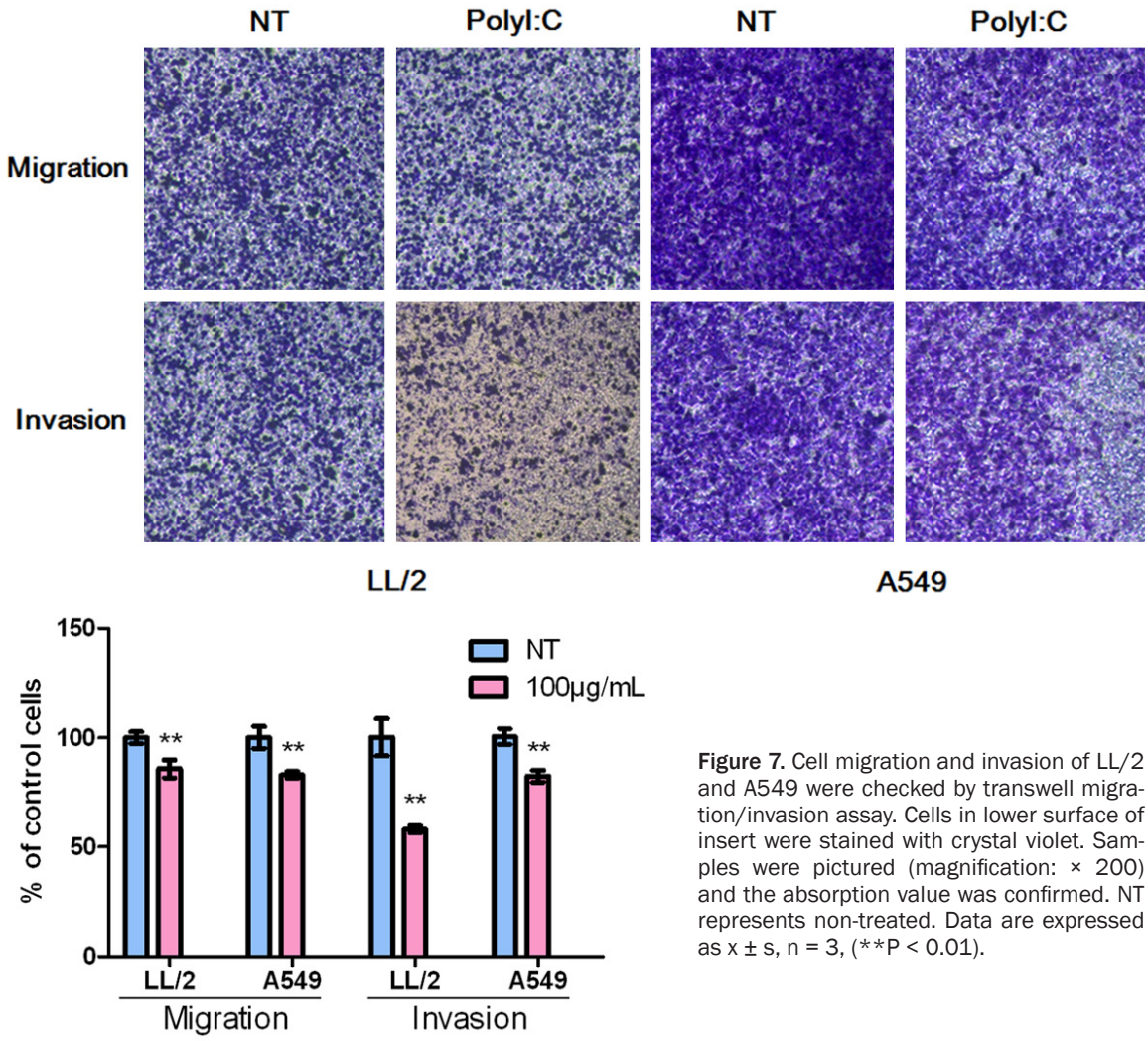

Figure 7. Cell migration and invasion of LL/2 and A549 were checked by transwell migration/invasion assay. Cells in lower surface of insert were stained with crystal violet. Samples were pictured (magnification: × 200) and the absorption value was confirmed. NT represents non-treated. Data are expressed as x ± s, n = 3, (**P < 0.01).

LL/2 subcutaneous transplanted tumor primarily metastasizes to the lung, then to the liver. Likewise, our H&E staining results further proved this. As illustrated in **Figure 11**, in terms of lung tissue, there existed a huge tumor metastasis loci in the PBS group and a smaller one in the both of PolyI:C inhale and PD1 groups while there was none in the lung of PolyI:C im group. However, PolyI:C im group has precursor of tumor formation. In addition, pulmonary edema, capillary hyperplasia around the metastasis, alveolar septal thickening and alveolar structure destruction were severe in the lungs of all groups. These developments can be seen in liver tissue H&E staining where small nodular cancer metastases were present in all groups except the PolyI:C im group. But the liver metastasis of the PD1 group was less than that of the PBS and the PolyI:C inhale groups, and the PolyI:C inhale group was less than the PBS group. In addition, no obvious metastases were seen in the four groups of brain tissues (images were taken at × 40 and × 200 magnification).

Influence of PolyI:C on survival time of transplanted tumor mice

To examine the speculated influence of polyI:C on anti-tumor and anti-metastasis, we further investigated its influence on survival time of LL/2 transplanted tumor mice. The log-rank analysis (**Figure 12**) showed that PolyI:C im and inhale groups prolonged mouse median survival to 44 days and 31 days, respectively, versus 25 days for the PBS group. In addition, survival time of the PD1 group was also significantly extended to 42 days. Therefore, it was illustrated that PolyI:C was obviously prolonged and

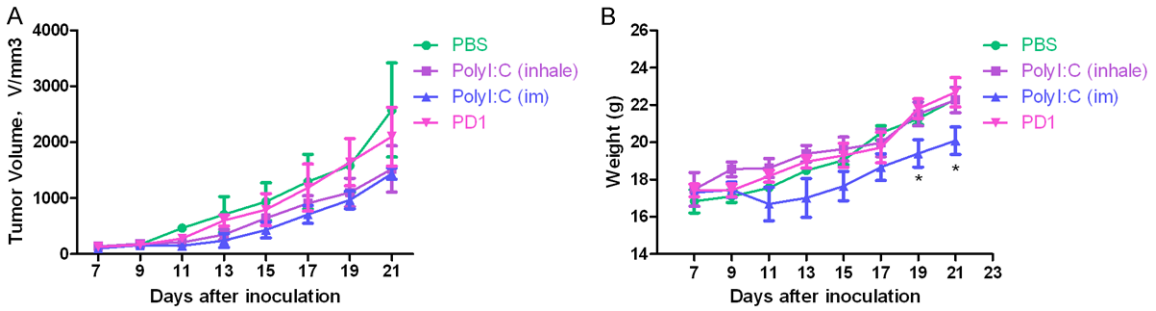

Figure 8. A. Tumor volume of mice transplanted tumor model changes over time during the experiment. B. Mice weight changes after inoculated LL/2 cells during the experiment. Data are expressed as x ± s, n = 6; *P < 0.05 versus the PBS group.

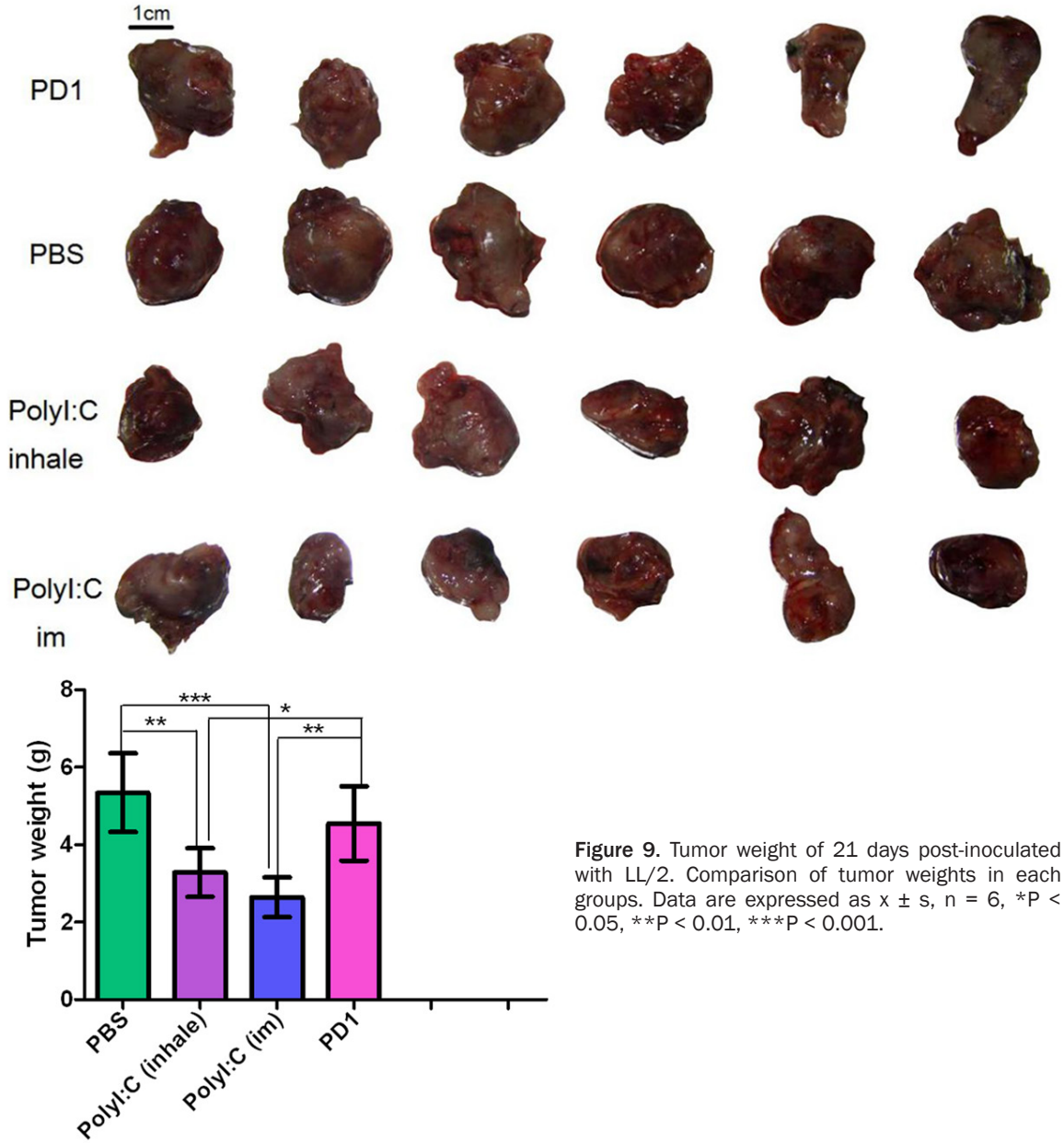

Figure 9. Tumor weight of 21 days post-inoculated with LL/2. Comparison of tumor weights in each groups. Data are expressed as x ± s, n = 6, *P < 0.05, **P < 0.01, ***P < 0.001.

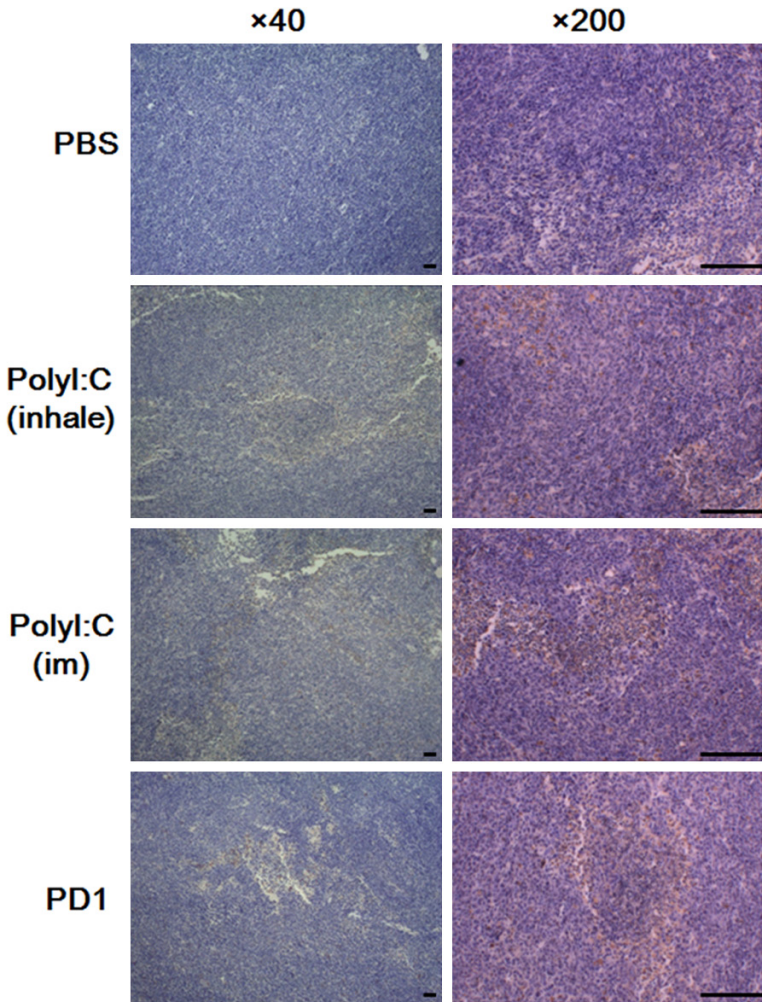

Figure 10. Observe tumor apoptosis. Paraffn-embedded tumor sections after TUNEL, scale bar = 120 μm, and the apoptotic cells shown in brown.

survival time of LL/2 transplanted tumor mice by im, even with a side effect of weight loss.

Influence of Polyl:C on CD80, CD86 of tumor-bearing mice

Dendritic cells (DCs) are extremely specialized antigen-presenting cells with the distinctive ability to establish and regulate primary immune responses [23]. The role of dendritic cells in presenting tumor antigens is very important in tumor immunity. The main purpose of inoculation of tumor vaccines is to enable tumor antigens to enter DCs and provide conditions for optimal maturation to become effective immune-stimulating APCs [24]. DCs capture and process antigens to present in the context of MHC molecules. Matured DCs up-regulate major histocompatibility complexes (MHC) I and II molecules and co-stimulatory molecules CD86 and CD80 as well as promotes tumor T cell infiltration [25]. Gavin *et al.* have suggested that engaging other pathogen-sensing receptors might be more useful in DC vaccination [26]. Enhanced stimulation of DC maturation by TLRs is a key issue in cancer immunotherapy [27].

Polyl:C is the ligand of TLR3 and many cytoplasmic RNA sensors in DC [28]. Polyl:C has been shown to promote maturation of human DC cells *in vitro*, suggesting that it is likely to be an adjuvant for DC-based immunotherapy. TLR3, the receptor for double-stranded RNA, binds to the cohesive protein TRIF. This pathway ultimately activates TRAF3 and IRF3, leads to the secretion of CD40, CD80, CD86 [29]. More studies have shown that Polyl:C can effectively up-regulate the MHC class I and class II, CD83, CD86 and CD40 molecules in healthy subjects and patients with stage III/IV ovarian cancer [30]. Therefore, we analyzed CD80 and CD86 of splenic DC cells in lung cancer-transplanted tumor model mice, and similar results were detected (**Figure 13**). As for the results regarding CD11c, the intramuscular Polyl:C group was 7.85% and the PBS group was 4.96%, while the positive rate of isotype control was 6.02%. Lung cancer may reduce the DC cells of spleen tissue, but Polyl:C up-regulated the DC cells of spleen tissue.

Then, we studied the positive rate and MFI of CD80 and CD86. From these results, we can see that the mice with lung cancer have increased CD80 and CD86 compared with the same type of contrast. When the CD80 positive rate and MFI of the isotype control were 0.25% and 68.49, respectively, the PBS group were raised to 13.60% and 785.9. However, the Polyl:C im group was 20.16% and 1210.76, significantly higher than the PBS group; the results for CD86 were the same. The CD80 positive rate and MFI of the isotype control were 0.73%

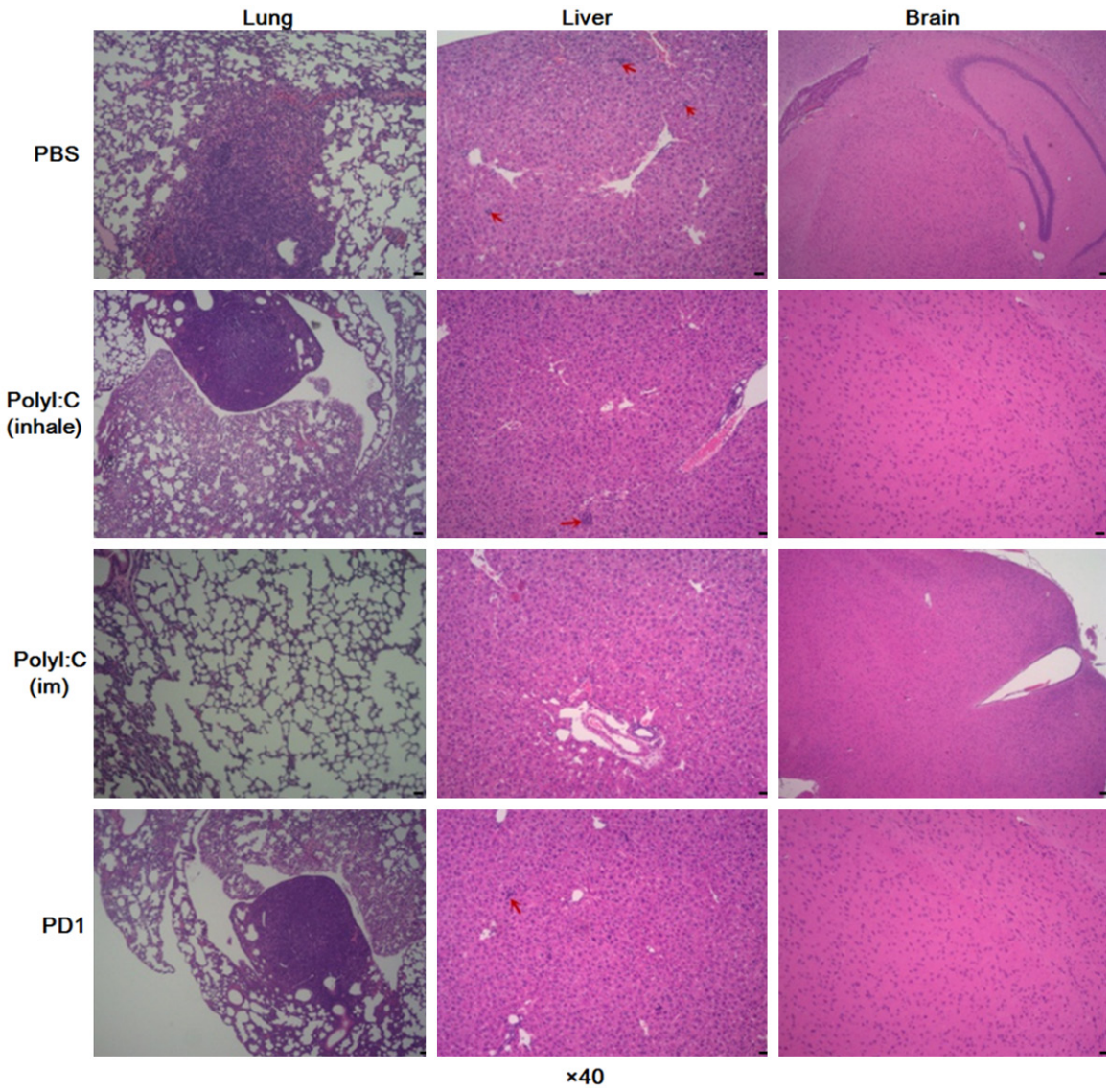

Figure 11. Observe the metastasis of various organs by H&E staining. Paraffn-embedded lung, liver, brain sections after H&E. Red arrows represent micrometastasis loci in liver. Images were taken at × 40 magnification, scale bar = 120 μm.

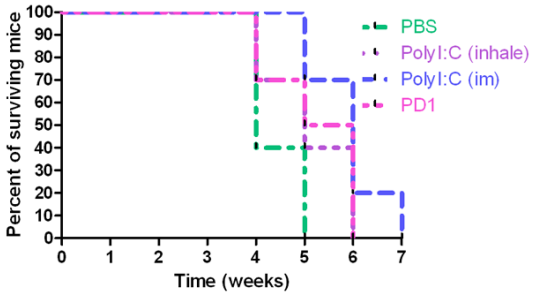

Figure 12. Kaplan-Meier survival curves of LL/2 transplanted tumor model. n = 10, *P < 0.05, PolyI:C inhale group versus the PBS group; ***P < 0.001, PolyI:C im group versus the PBS group.

and 135.97, the PBS group were 1.67% and 221.38, the PolyI:C im group were 4.01% and 353.20. In summary, the activation of TLR3 signaling with PolyI:C enhances DC maturation and up-regulated levels of MHC Class II, CD80 and CD86 molecules on DCs of spleen tissue further stimulated T cells *in vivo*.

Effect of PolyI:C on secretion of inflammatory cytokines in healthy mice

TLR3 signaling is known to utilize a MyD88-independent and NF-κB-dependent pathway, recruiting TRIF to activate TRAF6 and RIP1, and

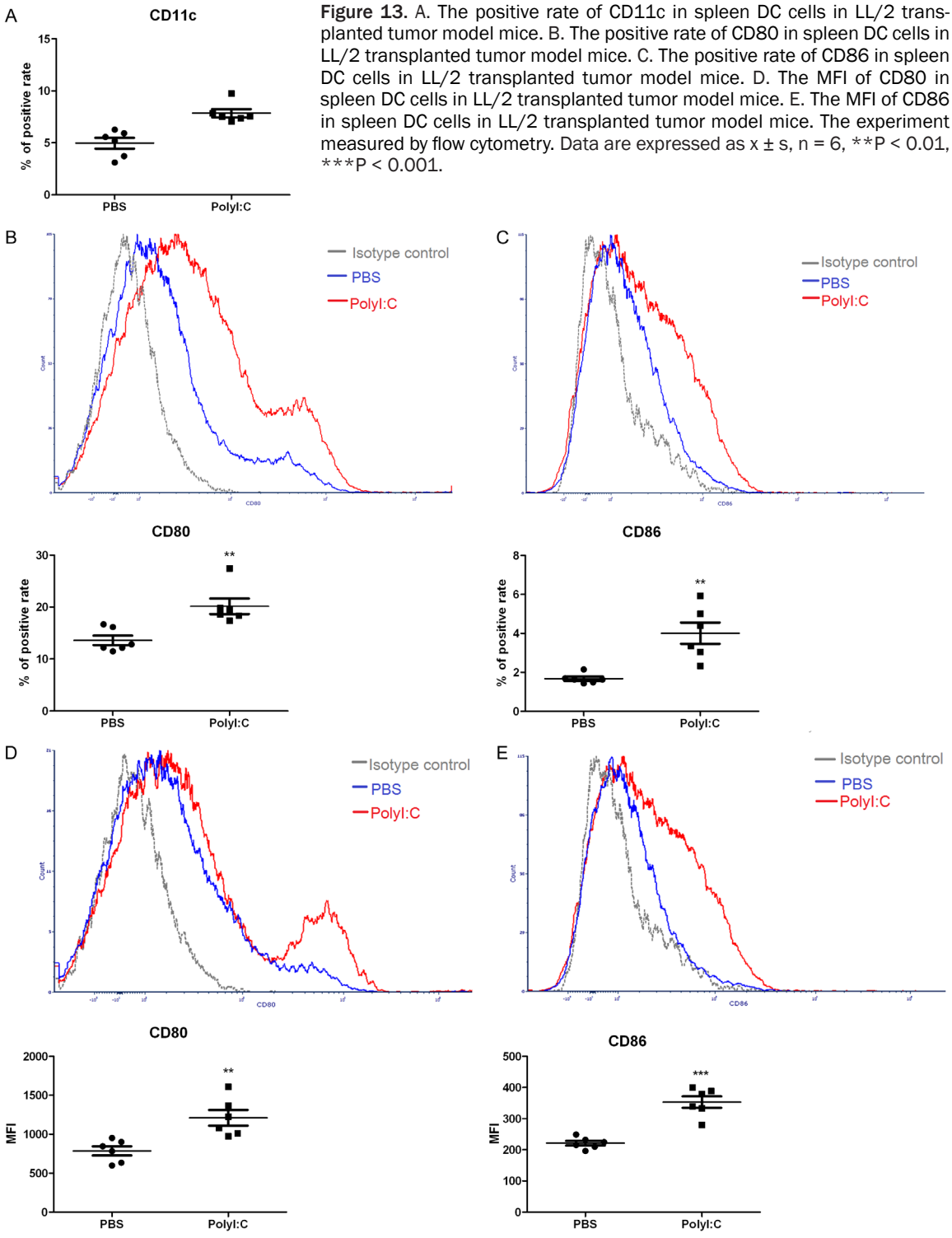

Figure 13. A. The positive rate of CD11c in spleen DC cells in LL/2 transplanted tumor model mice. B. The positive rate of CD80 in spleen DC cells in LL/2 transplanted tumor model mice. C. The positive rate of CD86 in spleen DC cells in LL/2 transplanted tumor model mice. D. The MFI of CD80 in spleen DC cells in LL/2 transplanted tumor model mice. E. The MFI of CD86 in spleen DC cells in LL/2 transplanted tumor model mice. The experiment measured by flow cytometry. Data are expressed as x ± s, n = 6, **P < 0.01, ***P < 0.001.

AP-1 activation involves TRAF6 and RIP1. Activated AP-1 secretes some inflammatory cytokines like TNF-α, and then recruits leukocytes, ultimately stimulates the anti-cancer immune responses [31, 32]. Therefore, we examined the effects of PolyI:C on cytokines in healthy mice to mitigate the effects of tumor microenvironment on cytokines. The results showed that the secretion of TNF-α, IL-2, IL-4, IL-6 caused a marked change after 2 h of PolyI:C-treated *in vivo*, especially for TNF-α and IL-6 **Figure 14**. Our results indicated that PolyI:C can induce a series of chemokines *in vivo* to enhance immune stimulation. TNF-α can also

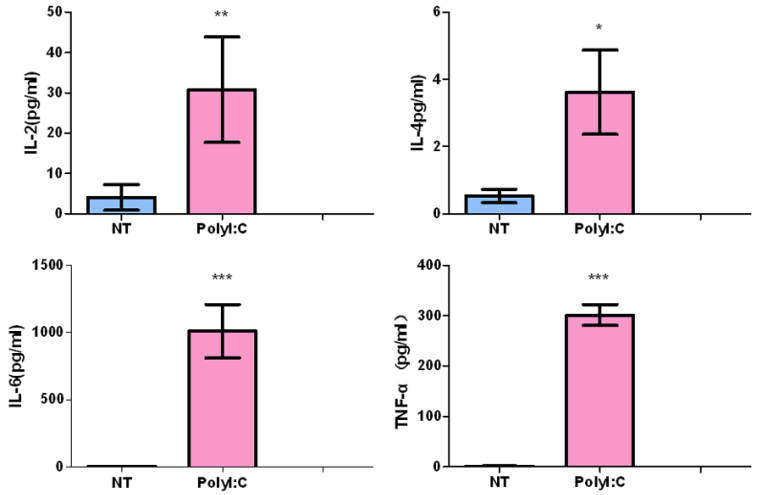

Figure 14. Changes of cytokines in healthy mice after 2 hours of PolyI:C administration. NT represents PBS administration. The experiment determined using Multiplex immunoassay. Data are expressed as x ± s, n = 3, *P < 0.05, **P < 0.01, ***P < 0.001.

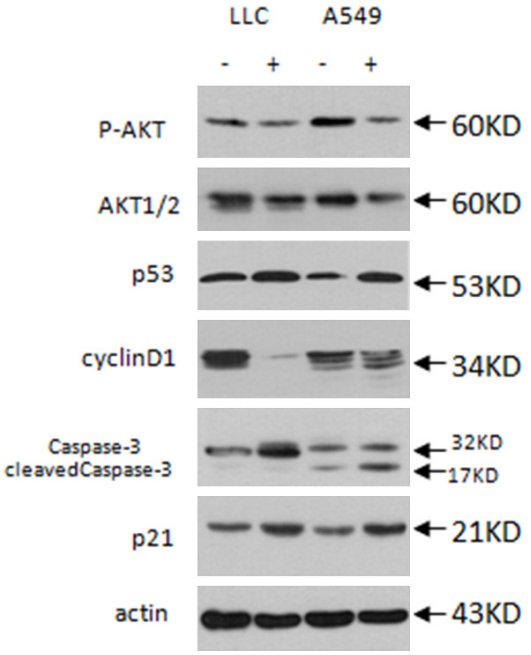

Figure 15. Using western blot analysis studied the expression of cell cycle and apoptosis-related proteins in LL/2 and A549 cell lines. - represents untreated, + represents treated with PolyI:C.

cause cancer cell apoptosis by inducing activation of caspase 7/3 [33].

PI3K/Akt/p53 pathway is involved in PolyI:C-induced anti-tumor effects

Studies have shown that TLR3 regulates NF-κB, MAPK and JAK-STAT signaling pathways in immune cells (**Figure 16**) [22, 34, 35]. In many malignant tumors, the PI3K/Akt pathway participated in multiple cellular functions, including cell growth, division, proliferation, anti-apoptosis, motility, invasion and intracellular trafficking [36]. Inhibition of Akt phosphorylation was reported to induce apoptosis and to have an effect on the cell cycle, thereby inhibiting tumor growth in NSCLC [19]. Findings by Harashima *et al.* demonstrated that TLR3 signaling inhibits proliferation and triggers apoptosis of prostate cancer cells partially through blocking of the PI3K/Akt pathway [37]. These data convinced our group to study whether the anti-tumor effect in NSCLC of PolyI:C is enhanced by inactivating the PI3K/Akt signaling pathway *in vitro* and in a transplanted tumor mouse model (**Figure 17**). We studied the influence of PolyI:C treatment on phosphorylation of Akt and found that, phosphorylation was inhibited both in LL/2 and A549 cells. PI3K/Akt/mTOR pathway increased expression of cyclinD1 [38]. Additionally, Akt suppresses the expression of p21 and p53, which also serve as negative regulators of the cell cycle [39, 40], then promotes the expression of cyclinD1 [41]. To clarify the potential molecular mechanisms of PolyI:C blocking G1 phase, we analyzed the expression of partial cycle-associated protein.

As **Figure 15** shows, after PolyI:C treated, the expression of protein p21 and p53 were increased, in contrast the cyclinD1 expression was inhibited. G1 phase progression is controlled by cyclinD1 [42]; PolyI:C blocked cells in the G1 phase by reducing cyclinD1, which consistent with the results of our cell cycle assay using flow cytometry. Akt prevents cancer cell death by reducing the expression of apoptotic precursors, such as p53 and caspase 3. We examined the expression of pro-apoptotic molecules in the presence and absence of PolyI:C. PolyI:C treatment promoted the expression of p53 and cleaved caspase3,and significant changes were observed in the expression of caspase 3 both in LL/2 and A549. This means PolyI:C can induce p53-caspase-dependenta-

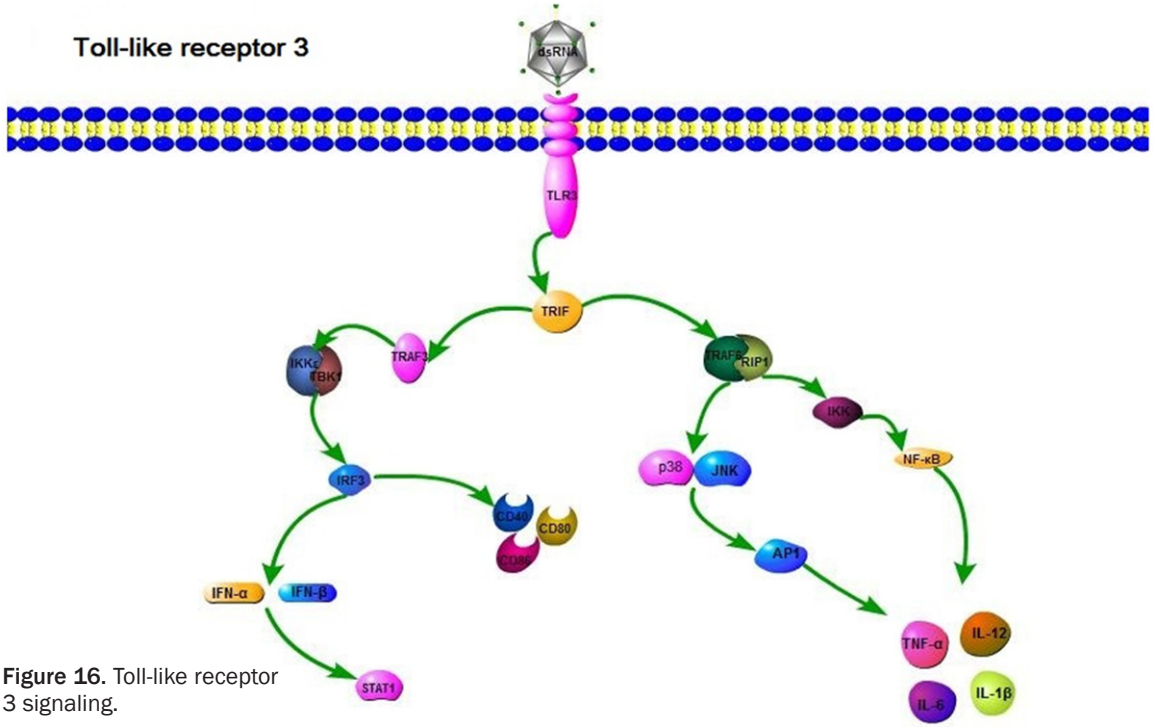

Figure 16. Toll-like receptor 3 signaling.

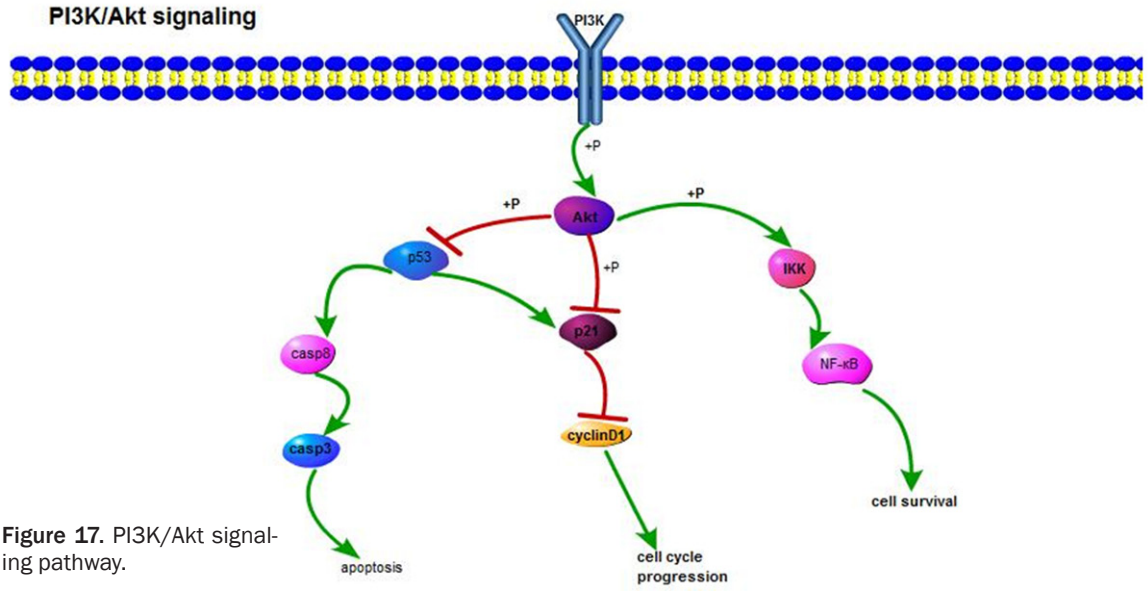

Figure 17. PI3K/Akt signaling pathway.

poptosis of LL/2 and A549,by reducing the expression of p-Akt.

The same results were obtained by immunohistochemistry and the positive staining area was calculated in **Figure 18**. The positive staining area of p-Akt and cyclinD1 in PolyI:C intramuscular group were reduced compared to the PBS group, while those for p53, p21 and caspase 3 were increased. In general, PolyI:C treatment regulated PI3K/Akt/p53 signaling pathway and changed the expression patterns of cell death- and proliferation-related molecules consistent with apoptosis and growth stagnation.

Conclusions

In summary, PolyI:C is an effective immunemodulator. We used LL/2 and human NSCLC cells A549 to determine the antitumor effect of

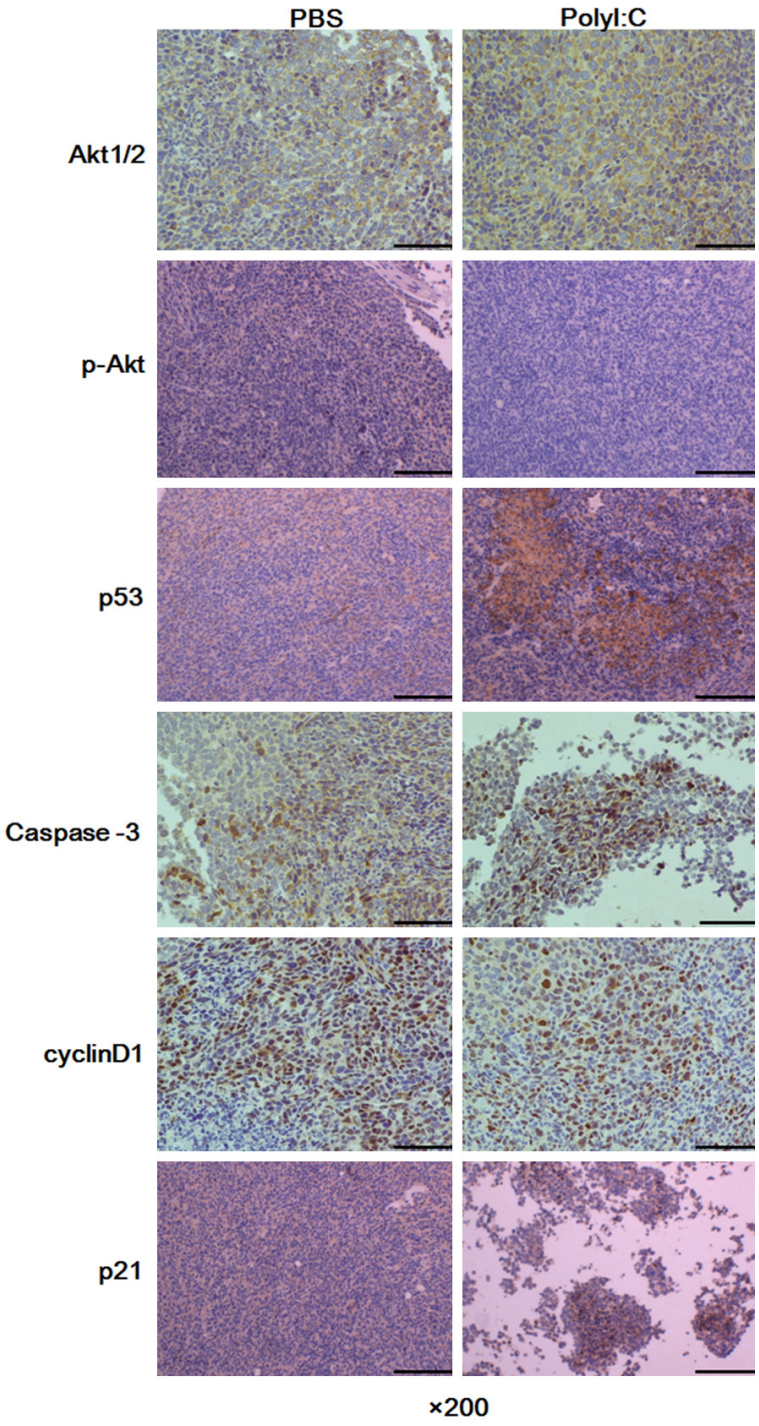

Figure 18. Using immunohistochemical analysis studied the expression of cell cycle and apoptosis-related proteins in tumor tissues. Images were taken at × 200 magnification.

Polyl:C *in vitro*, and *in vivo* using the LL/2 murine lung cancer model. Polyl:C effectively impacts on cellular proliferation, migration and invasion, G1 phase blocking and apoptosis in LL/2 and A549 cancer cells by regulating Akt and downstream molecules *in vitro*. More importantly, it significantly suppressed tumor development and metastasis, prolonged survival times, up-regulated levels CD80 and CD86 molecules of LL/2 tumor-bearing mice, although there was a side effect of weight loss. Toll-like receptor research could lead to a new form of cancer immunotherapy. Therefore, a better understanding of the mechanism of Polyl:C in NSCLC as a potential anti-tumor agent is essential.

Acknowledgements

This work was financially supported by National Natural Science Foundation of China (Grant No. 81160291), Basic Medical Research Service Project of Chinese Academy of Medical Sciences (Grant No. 2018PT35002) and CAMS Innovation Fund for Medical Sciences (Grant No. 2017-I2M-1-011).

Disclosure of conflict of interest

None.

Abbreviations

NSCLC, non-small-cell lung carcinoma; Polyl:C, polyinosinic-polycytidylic acid; TLR3, toll like receptor 3; APC, antigen presenting cell; IRF, interferon regulatory factors; DC, dendritic cell; FBS, fetal bovine serum; OD, optical density value; PI, propidium iodide; PBS, phosphate buffer saline; IL2, interleukin 2; IL4, interleukin 4; IL6, interleukin 6; TNF-α, tumor necrosis factorα; MDA5, melanoma differentiation associated gene 5; TUNEL, terminal deoxynucleotidyl transferase-mediated dUTP-biotin nick end labeling assay.

Address correspondence to: Zhonggao Gao, State Key Laboratory of Bioactive Substance and Function of Natural Medicines, Institute of Materia Medica, Chinese Academy of Medical Sciences and Peking Union Medical College, 1 Xian Nong Tan Street, Beijing 100050, China. E-mail: zggaoimm@126.com; Changshan An, Department of Respiratory Medicine, Affiliated Hospital of Yanbian University, Yanji 133000, Jilin, China. E-mail: cs_an2003@163.com

References

[1] National Comprehensive Cancer Network. NCCN clinical practice guidelines in oncology: non-small cell cancer guidelines. V4.2015. Available at: http://www.nccn.org/professionals/physician_gls/pdf/nscl.pdf. Accessed 19 February, 2014.

[2] Gettinger S, Lynch T. A decade of advances in treatment for advanced non-small cell lung cancer. Clin Chest Med 2011; 32: 839-851.

[3] Vesely MD, Kershaw MH, Schreiber RD, Smyth MJ. Natural innate and adaptive immunity to cancer. Annu Rev Immunol 2011; 29: 235-271.

[4] Liu Y, Zeng G. Cancer and innate immune system interactions: translational potentials for cancer immunotherapy. Immunother 2012; 35: 299-308.

[5] Akira S, Takeda K. Toll-like receptor signalling. Nat Rev Immunol 2004; 4: 499-511.

[6] Ridnour LA, Cheng RY, Switzer CH, Heinecke JL, Ambs S, Glynn S, Young HA, Trinchieri G, Wink DA. Molecular pathways: toll-like receptors in the tumor microenvironment-poor prognosis or new therapeutic opportunity. Clin. Cancer Res 2013; 19: 1340-1346.

[7] Ito T, Amakawa R, Fukuhara S. Roles of Toll-like receptors in natural interferon-producing cells as sensors in immune surveillance. Hum Immunol 2002; 63: 1120-1125.

[8] Pisetsky DS, Gauley J, Ullal AJ. HMGB1 and microparticles as mediators of the immune response to cell death. Antioxid. Redox Sign 2011; 15: 2209-2219.

[9] Estornes Y, Toscano F, Virard F, Jacquemin G, Pierrot A, Vanbervliet B, Bonnin M, Lalaoui N, Mercier-Gouy P, Pachéco Y, Salaun B, Renno T, Micheau O, Lebecque S. dsRNA induces apoptosis through an atypical death complex associating TLR3 to caspase-8. Cell Death Differ 2012; 19: 1482-1494.

[10] Shatz M, Menendez D, Resnick MA. The human TLR innate immune gene family is differentially influenced by DNA stress and p53 status in cancer cells. Cancer Res 2012; 72: 3948-3957.

[11] Paone A, Starace D, Galli R, Padula F, De Cesaris P, Filippini A, Ziparo E, Riccioli A. Toll-like receptor 3 triggers apoptosis of human prostate cancer cells through a PKC-alpha-dependent mechanism. Carcinogenesis 2008; 29: 1334-1342.

[12] Salaun B, Coste I, Rissoan MC, Lebecque SJ, Renno T. TLR3 can directly trigger apoptosis in human cancer cells. Immunol 2006; 176: 4894-4901.

[13] Van DN, Roberts CF, Marion JD, Lépine S, Harikumar KB, Schreiter J, Dumur CI, Fang X, Spiegel S, Bell JK. Innate immune agonist, dsRNA, induces apoptosis in ovarian cancer cells and enhances the potency of cytotoxic chemotherapeutics. FASEB J 2012; 26: 3188-3198.

[14] Inao T, Harashima N, Monma H, Okano S, Itakura M, Tanaka T, Tajima Y, Harada M. Antitumor effects of cytoplasmic delivery of an innate adjuvant receptor ligand, polyI:C, on human breast cancer. Breast Cancer Res Treat 2012; 134: 89-100.

[15] Nomi N, Kodama S, Suzuki M. Toll-like receptor 3 signaling induces apoptosis in human head and neck cancer via survivin associated pathway. Oncol 2010; 24: 225-231.

[16] Levitzki A. Targeting the immune system to fight cancer using chemical receptor homing vectors carrying polyinosine/cytosine (PolyIC). Front Oncol 2012; 2: 1-10.

[17] Shatz M, Menendez D, Resnick MA. The human TLR innate immune gene family is differentially influenced by DNA stress and p53 status incancer cells. Cancer Res 2012; 72: 3948-3957.

[18] Harashima N, Inao T, Imamura R, Okano S, Suda T, Harada M. Roles of the PI3K/Akt pathway and autophagy in TLR3 signaling-induced apoptosis and growth arrest of human prostate cancer cells. Cancer Immunol Immunother 2012; 61: 667-676.

[19] Lin SL, Greene JJ, Ts'o PO, Carter WA. Sensitivity and resistance of human tumor cells to interferon and rIn. rCn. Nature 1982; 297: 417-419.

[20] Chawla-Sarkar M, Lindner DJ, Liu YF, Williams BR, Sen GC, Silverman RH, Borden EC. Apoptosis and interferons: role of interferon-stimulated genes as mediators of apoptosis. Apoptosis 2003; 8: 237-249.

[21] Hanahan D, Weinberg Robert A. Hallmarks of cancer: the next generation. Cell 2011; 144: 646-674.

[22] Lau WH, Zhu XG, Ho SWT, Jeak LD. Combinatorial treatment with polyI:C and anti-IL6 enhances apoptosis and suppresses metastasis of lung cancer cells. Oncotarget 2017; 8: 32884-32904.

[23] Banchereau J, Briere F, Caux C, Davoust J, Lebecque S, Liu YJ, Pulendran B, Palucka K. Immunobiology of dendritic cells. Annu Rev Immunol 2000; 18: 767-811.
[24] Gilboa E. DC-based cancer vaccines. Clin Invest 2007; 117: 1195-1203.
[25] Sousa CR. Dendritic cells in a mature age. Nat Rev Immunol 2006; 6: 476-483.
[26] Amanda L. Gavin, Kasper Hoebe, Bao Duong, Ota T, Martin C, Beutler B, Nemazee D. Adjuvant-enhanced antibody responses in the absence of toll-like receptor signaling. Science 2016; 314: 1936-1938.
[27] Scholch S, Rauber C, Weitz J, Koch M, Huber PE. TLR activation and ionizing radiation induce strong immune responses against multiple tumor entities. Oncoimmunology 2015; 4: e1042201.
[28] Matsumoto M, Seya T. TLR3: interferon induction by double-stranded RNA including PolyI:C. Adv Drug Deliv Rev 2008; 60: 805-812.
[29] Takeda K, Akira S. TLR signaling pathways. Semin Immunol 2004; 16: 3-9.
[30] Navabi H, Jasani B, Reece A, Clayton A, Tabi Z, Donninger C, Mason M, Adams M. A clinical grade poly I:C-analogue (Ampligen) promotes optimal DC maturation and Th1-type T cell responses of healthy donors and cancer patients in vitro. Vaccine 2009; 27: 107-115.
[31] Meylan E, Burns K, Hofmann K, Blancheteau V, Martinon F, Kelliher M, Tschopp J. RIP1 is an essential mediator of toll-like receptor 3-induced NF-kappa B activation. Nat Immunol 2014; 5: 503-507.
[32] Galli R, Starace D, Busà R, Angelini DF, Paone A, De Cesaris P, Filippini A, Sette C, Battistini L, Ziparo E, Riccioli A. TLR stimulation of prostate tumor cells induces chemkine-mediated recruitment of specific immune cell types. Immunol 2010; 184: 6658-6669.
[33] Daniel D, Wilson NS. Tumor necrosis factor: Renaissance as a cancer therapeutic? Curr Cancer Drug Tar 2008; 8: 124-131.
[34] Zhang X, Xu J, Ke X, Zhang S, Huang P, Xu T, Huang L, Lou J, Shi X, Sun R, Wang F, Pan S. Expression and function of Toll-like receptors in peripheral blood mononuclear cells from patients with ovarian cancer. Cancer Immunol Immunother 2015; 64: 275-286.
[35] Matijevic Glavan T, Cipak Gasparovic A, Vérillaud B, Busson P, Pavelic J. Toll-like receptor 3 stimulation triggers metabolic reprogramming in pharyngeal cancer cell line through Myc, MAPK, and HIF. Mol Carcinog 2017; 56: 1214-1226.
[36] Pérez-Ramírez C, Cañadas-Garre M, Molina MÁ, Faus-Dáder MJ, Calleja-Hernández MÁ. PTEN and PI3K/AKT in non-small-cell lung cancer. Pharmacogenomics 2015; 16: 1843-1862.
[37] Qie S, Diehl JA. Cyclin D1, Cancer progression and opportunities in cancer treatment. Mol Med (Berl) 2016; 94: 1313-1326.
[38] Kumar R, Hung MC. Signaling intricacies take center stage in cancer cells. Cancer Res 2005; 65: 2511-2515.
[39] Abraham AG, O'Neill E. PI3K/Akt-mediated regulation of p53 in cancer. Biochem Soc Trans 2014; 42: 798-803.
[40] Muise-Hemericks RC, Grimes H, Bellacosa A, Malstrom SE, Tsichlis PN, Rosen N. Cyclin D expression is controlled post-transcriptionally via a phosphatidylinositol 3-kinase/Aedepndent pathway. Biol Chem 1998; 273: 29864-29872.
[41] Liao K, Li J, Wang Z. Dihydroartemisinin inhibits cell proliferation via AKT/GSK3β/cyclinD1 pathway and induces apoptosis in A549 lung cancer cells. Int J Clin Exp Pathol 2014; 7: 8684-8691.
[42] Ogawara Y, Kishishita S, Obata T, Isazawa Y, Suzuki T, Tanaka K, Masuyama N, Gotoh Y. Akt enhances Mdm2-mediated ubiquitination and degradation of p53. Biol Chem 2002; 277: 21843-21850.